Performance Analysis of RF/VLC Enabled UAV Base Station in Heterogeneous Network

Yash Gupta, Mansi Peer, Vivek Ashok Bohara
WiroComm Research Group, Department of ECE, IIIT-Delhi, India
Email: {yash17210, mansip, vivek.b}@iiitd.ac.in

***Abstract*—In this paper, we study the trade-offs between two network configurations employed in a heterogeneous network setup wherein unmanned aerial vehicle (UAV) base stations (UBS) coexist with a macro base station (MBS). Specifically, two network configurations are investigated: (i) Heterogeneous network with MBS and UAV-Cellular base station (UAV-CBS) and (ii) Heterogeneous network with MBS and visible light communication (VLC) enabled UAV-Optical base station (UAV-OBS). A framework has been developed to compare the average spectral efficiency of the proposed network configurations. In the developed framework, the average spectral efficiency has been analyzed by taking into account the user's association and user's quality of service (QoS) requirement and location. To gain more concrete insights, we compare the above configurations for (i) one UBS and one MBS network, and (ii) two UBSs and one MBS network. We infer, from the simulation results, that as the number of UBSs in use increases, the network with VLC enabled UAV-OBS outperforms the cellular-enabled UAV-CBS.**

***Index Terms*—UAV Base Station, Visible Light Communication, Heterogeneous network**

I. INTRODUCTION

Ultra-reliable low latency communication (URLLC), massive connectivity, desirable quality-of-service (QoS), and high-speed uplink and downlink are essentials of the fifth-generation (5G) and beyond wireless networks. With the exponential increase in user-equipment's (UEs) density and the demand for better connectivity, the present terrestrial infrastructure seems insufficient. Recently, the use of unmanned aerial vehicles (UAVs) has increased in verticals such as security and defense [1]. Utilizing the UAVs as aerial base stations looks like a promising solution that can improve the network's agility. UAVs also have several key potential applications in wireless systems with their inherent attributes such as mobility, flexibility, and adaptive altitude. This emerging technology not only helps in providing reliable but also cost-effective wireless connectivity for ground users [2]. Some of the prominent use-cases of the UAV Base Stations(UBSs) are during disasters such as floods and earthquake, which affects the accessibility of ground base stations (BSs). Further, in cases of unusual excessive demands in some areas, such as during an outdoor concert, UBSs can complement the terrestrial network without deployment of additional permanent infrastructure.

To reap the benefits of deploying UAVs as aerial base stations, researchers are working to address prominent technical challenges such as placement, air-to-ground channel modeling, user association, and flight time optimization. For instance, in [3], the authors studied the efficient deployment of aerial base stations to maximize the coverage and rate performance of wireless networks. The work in [4] performed air-to-ground channel modeling for UAV-based communications. The work in [5] studied the joint optimization of user scheduling and UAV trajectory to maximize users' minimum rate. The work in [6] investigated the area to UAV assignment for capacity enhancement of heterogeneous wireless networks.

In cases where UBSs share the same allocated cellular spectrum as the macro-base station (MBS), the optimal resource allocation between the two BS is a major concern. This goes hand-in-hand with optimal UBS placement to ensure better frequency reuse and thus improved spectral efficiency. The scarcity of spectrum, cost, and interference in traditional radio frequency (RF) has motivated the network operators to exploit higher frequencies such as visible light communication (VLC) for cellular transmissions [7]. VLC possesses several interesting features such as higher data rate, higher energy efficiency, lower battery consumption, and reduced latency addresses some of the requirements of evolving 5G/Beyond 5G systems [8]. Modern VLC systems based on intensity modulation (IM) and direct detection (DD) with optical orthogonal frequency division multiplexing (OFDM) have been shown to achieve data rates in the range of Gbps [9]. Integrating visible light communication (VLC) with conventional cellular-enabled wireless networks has been shown to improve the achievable data rates of mobile users. It is a known fact that the received power, in VLC, depends heavily on the line of sight (LOS) signals that may get blocked due to the limited field-of-view (FOV) of the receivers, and/or irradiance angle of the optical LEDs. As such, the dense deployment of LEDs may not guarantee reliable coverage. VLC is thus considered as a complementary rather than substituting technology to RF [10]. Consequently, a very intuitive approach to solve the issue of bandwidth scarcity and allocation in UBS-MBS heterogeneous networks is to use UAVs as optical base stations. UAVs may now be used as VLC-transmitter and provide service to the users within the field-of-view (FOV).

While most of the prior literature provides a comprehensive overview of the working of standalone UAV base stations, there is no significant work discussing the performance of RF/VLC Enabled UAV base stations in the heterogeneous network. In this paper, we bridge this gap by studying the trade-offs between two network configurations employed in a heterogeneous network setup wherein a UAV base station coexist with the MBS. In particular, the main contributions of the paper are as follows:

- We illustrate the advantage of using VLC-enabled UAV base station in the heterogeneous network.
- We propose a framework to optimally utilize a co-existing multi-UAV heterogeneous network to maximize average spectral efficiency. Thus, addressing the issue of limited licensed spectrum along with ensuring good QoS.
- The performance of the heterogeneous network has been analyzed, via simulations, by taking into account the user's association, QoS requirement and location.

The rest of the paper is organized as follows. Section II describes the system model of the network. The channel model and SNR model are also presented. User association and UBS placement strategy are discussed in section III. Section IV discusses various simulation results for the framework proposed. We conclude the paper in section V.

II. System Model

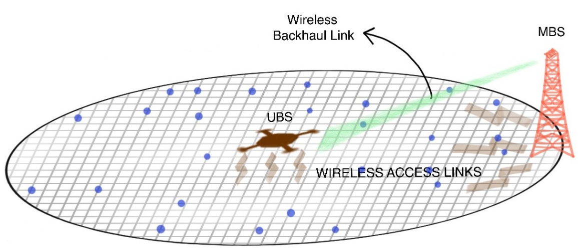

Figure 1. UBSs assisted heterogeneous network architecture.

The system model consists of one UBS, one terrestrial MBS, and user equipments (UEs) on the ground as shown in Fig.1. We assume that there exists a free-space optical (FSO) link for wireless backhauling from MBS to UBS [11]. Traditional RF communications are used as the wireless access solution in the case of heterogeneous UAV-CBS and MBS network. VLC access links are being exploited for the case of UAV-OBS. Here, we assume that the bottleneck of transmitting data from the MBS to UEs via UBS is the channel between UBS and UEs. Let the horizontal (on-ground) distance between the UBS at coordinates (x_u,y_u,h_u) and a random UE $\mathcal{U}_i$ at coordinates (x_i^{pos}, y_i^{pos}) be g_i. Hence, the 3D distance between the UBS and $\mathcal{U}_i$ can be expressed as :

$$d_i^u = \sqrt{{g_i}^2 + h_u^2} \qquad \text{where}$$
$$g_i = \sqrt{(x_u - x_i^{pos})^2 + (y_u - y_i^{pos})^2}.$$

$$\text{Similarly,} \qquad d_i^m = \sqrt{{p_i}^2 + h_m^2} \qquad \text{where}$$
$$p_i = \sqrt{(x_m - x_i^{pos})^2 + (y_m - y_i^{pos})^2}. \tag{1}$$

where (x_m,y_m,h_m) are the coordinates defining the fixed location of the MBS. Thus, d_i^m is the 3D distance between MBS and $\mathcal{U}_i$. All the UEs are allowed to associate with either MBS or UBS. The association is based on maximum instantaneous received SNR. Thus, the association model depends on the channel between UBS and MBS. We have an cellular channel in the case of UAV-CBS and a VLC channel in the case of UAV-OBS. The channel models are discussed in subsequent subsections.

The wireless propagation channel between the UBS and the UEs can be divided into two scenarios, i.e., the links can either be in line-of-sight (LOS) or non-line-of-sight (NLOS). The probability of having LOS between the UBS and the UEs can be modeled as [12]

$$\begin{aligned} \rho_i =& \frac{1}{1 + \alpha e^{-\beta(\theta_i - \alpha)}} \\ =& \frac{1}{1 + \alpha e^{-\beta\left(\frac{180}{\pi}\arctan\left(\frac{h_u}{g_i}\right) - \alpha\right)}} \end{aligned} \tag{2}$$

where θ_i is the elevation angle between the UBS and location (x_i^{pos}, y_i^{pos}), α and β are the environmental parameters. Intuitively, in the NLOS scenario, UEs can still communicate with the UBS but suffer from much stronger reflections and diffractions.

A. Channel Model

Using the probability of wireless channel being in LOS/NLOS, as discussed above, we can now define both cellular and VLC channel models as described below.

- Cellular channel model :
  Let η_i^u be the average pathloss (in dB) between the UAV-CBS and UE and η_i^m be the average pathloss (in dB) between the MBS and UE. Thus,

$$\eta_i^u = 20\log_{10}\left(\frac{4\pi f_c d_i^u}{c}\right) + \rho_i \xi^{los} + (1 - \rho_i)\,\xi^{nlos}$$

$$\eta_i^m = 20\log_{10}\left(\frac{4\pi f_c d_o^m}{c}\right) + 20n\log_{10}\left(\frac{d_i^m}{d_o^m}\right) \tag{3}$$

  Here, ξ_{los} and ξ_{nlos} are the average additional pathloss for LOS and NLOS scenario respectively. Generally, $\xi_{nlos} \geq \xi_{los}$. d_o^m is the free space reference distance and ρ_i is as defined in (2).

- VLC channel model :
  For the standard static VLC channel, the following model is employed [13]. H_{LOS} is the channel gain of LoS component, which is given as:

$$H_{LOS} = \begin{cases} \dfrac{(m+1)A}{2\pi D_d^2}\cos^m(\phi)T_s(\psi)g(\psi)\cos(\psi) \\ \qquad\qquad 0 \leq \psi \leq \psi_c \ , \end{cases} \tag{4}$$

where m represents Lambertian order, A defines the physical area of the photodetector (PD), D_d is the distance between the transmitter LED and the PD. ψ and ϕ are the angle of incidence and angle of irradiance respectively, ψ_c is the receiver field of view (FOV), $T_s(\psi)$ and $g(\psi)$ are the gain of the optical filter and optical concentrator respectively. H_{NLOS}, the diffuse channel gain, due to NLoS path is given as:

$$H_{NLOS} = \frac{A_R}{A_{room}} \frac{\varrho}{1-\bar{\varrho}} \ , \tag{5}$$

where ϱ represents an instantaneous reflectance, $\bar{\varrho}$ an average reflectance. NLoS rays are reflected inside the room from the wall with A_R as the area of reflection point. A_i is the area of i_{th} grid on the wall and A_{room} is the total area of the room. For a given transmission power P_T, the total received power including diffused path through the walls can be obtained as:

$$P_r = \left[P_T H_{LOS} + \int_{walls} P_T H_{NLOS} \right] \tag{6}$$

B. SNR model

The UEs experience different received SNR while associating with the different base stations. Using the above-described channel models, we now describe the received SNR model for UEs. Assuming additive white Gaussian noise (AWGN) channel, such that for transmit signal x, the received signal is given as $y = Hx + n_1$, where $n_1 = \mathcal{CN}(0, \sigma_1^2)$ and H is channel gain, equivalent to the reciprocal of the pathloss.

- For UEs associated with MBS :
  Let γ_i^m denote the received SNR for a random user $\mathcal{U}_i$

$$\gamma_i^m = \frac{p^m 10^{\frac{-\eta_i^m}{10}}}{\sigma_1^2} \tag{7}$$

  where p^m is the transmission power of the MBS. $10^{\frac{-\eta_i^m}{10}}$ represents the channel gain. η_i^m is as defined in (3).

- For UEs associated with UAV-CBS :
  Let γ_i^{u1} denote the received SNR for a random user $\mathcal{U}_i$ associted with UAV-CBS.

$$\gamma_i^{u1} = \frac{p^u 10^{\frac{-\eta_i^u}{10}}}{\sigma_1^2} \tag{8}$$

  where p^u is the transmission power of the UAV-CBS. $10^{\frac{-\eta_i^u}{10}}$ represents the channel gain. η_i^u is as defined in (3).

- For UEs associated with UAV-OBS :
  We have used OOK modulation in the VLC link [14]. OOK is one of the standard modulation schemes defined in the VLC standard (IEEE 802.15.7). For the optical signal, with transmit power P_T, the detected electrical signal is filtered out at the receiver and the received signal, is given by:

$$y = \mathcal{R}P_r + n_2,$$

  where R is photodiode responsivity, $n_2 = \mathcal{CN}(0, \sigma_2^2)$ such that $\sigma_2^2 = \sigma_{shot}^2 + \sigma_{thermal}^2$ and P_r is total received power, as given in (6). Let γ_i^{u2} denote the received SNR for a random user $\mathcal{U}_i$ associated with UAV-OBS.

$$\gamma_i^{u2} = \frac{(\mathcal{R}P_r)^2}{\sigma_2^2} \tag{9}$$

III. User-association and UBS placement strategy

Utilizing the above discussed channel and SNR models, for all possible associations, we can now describe the strategy followed for user association for the two network configurations in consideration followed by respective UAV placement strategy.

A. Heterogeneous network with MBS and UAV-CBS

Given the location of UAV-CBS (x_u,y_u,h_u) and MBS(x_m,y_m,h_m), we can divide all the UEs into two sets. Let $\mathcal{A}_u$ and $\mathcal{A}_m$ be the sets consisting of the UEs associated with UAV-CBS and MBS respectively. For a random UE $\mathcal{U}_i$ at location (x_i^{pos}, y_i^{pos}),

$$\mathcal{U}_i \quad \epsilon \quad \begin{cases} \mathcal{A}_u & : \gamma_i^m < \gamma_i^{u1} \\ \mathcal{A}_m & : \gamma_i^m \geq \gamma_i^{u1}. \end{cases} \tag{10}$$

where γ_i^m and γ_i^{u1} are as defined in (7) and (8) respectively. Now, with knowledge of the sets $\mathcal{A}_m$ and $\mathcal{A}_u$ as described above, we describe the method to place the UAV-CBS to maximize the average spectral efficiency for all the UEs. The optimization problem to maximize average spectral efficiency can be defined as :

$$\arg\max_{x_u, y_u} \frac{\mathbf{n}(\mathcal{A}_m) \times \varphi_i^m + \mathbf{n}(\mathcal{A}_u) \times \varphi_i^u}{\mathbf{n}(\mathcal{A}_m) + \mathbf{n}(\mathcal{A}_u)} \tag{11}$$

where $\mathbf{n}(x)$ denote the cardinality of set x. φ_i^{u1}= $\log_2\left(1+\gamma_i^{u1}\right)$ and φ_i^m= $\log_2\left(1+\gamma_i^m\right)$ are the received spectral efficiency for a user associated to UAV-CBS and MBS respectively. It may be noted that (11) is indirectly a function of the sum of distances between UEs and UAV-CBS/MBS. The MBS is stationary and the UAV-CBS is located at a fixed height (h_u), the above problem essentially reduces to :

$$\arg\min_{x_u, y_u} \sum_{i \in \mathcal{A}_u} d_i^u \quad ; \qquad \arg\min_{x_u, y_u} \sum_{i \in \mathcal{A}_u} g_i^u \tag{12}$$

which gives the solution that UAV-CBS must be at the centroid of the location of all the UEs $\mathcal{U}_i \ \epsilon \ \mathcal{A}_u$. The updated coordinates of the UAV-CBS can thus be written as :

$$(x_u^{new}, y_u^{new}, h_u^{new}) = \left(\frac{\sum\limits_{i \in \mathcal{A}_u} x_i^{pos}}{\mathbf{n}(\mathcal{A}_u)}, \frac{\sum\limits_{i \in \mathcal{A}_u} y_i^{pos}}{\mathbf{n}(\mathcal{A}_u)}, h_u \right) \tag{13}$$

B. Heterogeneous network with MBS and UAV-OBS.

For this network configuration, it is assumed that UE needs to be in the FOV of the UAV-OBS to be able to associate with the same. Further, the probability of the UE being in LOS of the UAV-OBS must be greater than the threshold Γ.

Let $\mathcal{A}_u$ and $\mathcal{A}_m$ be the sets consisting of the UEs associated with UAV-OBS and MBS respectively. For a random UE $\mathcal{U}_i$ at location (x_i^{pos}, y_i^{pos}),

$$\mathcal{U}_i \quad \epsilon \quad \begin{cases} \mathcal{A}_u & : d_i^u < h_u \tan(\phi), \quad \rho_i > \Gamma \text{ and } \gamma_i^{u2} \geq \gamma_i^m \\ \mathcal{A}_m & : \text{otherwise.} \end{cases} \tag{14}$$

where γ_i^m and γ_i^{u2} are as defined in (7) and (9) respectively. d_i^u and p_i are as defined in (1) and (2) respectively.

Contrary to RF, VLC is susceptible to blockages (walls, human, material objects, etc.) thus naturally confined to a small area. It's thus easier to intuitively find the coverage region of the VLC. As per (2), the probability of a random UE being in a LOS of the UAV-OBS depends inversely on the on-ground distance between UE and UAV-OBS. Thus, farther the UE, lesser is the probability of being in LOS, smaller is the association probability with UAV-OBS. Thus, the UEs associated with the UAV-OBS using the VLC channel will be densely located near the center of the circle, with UAV-OBS as the center. On average, the circular area with some fixed radius r will have UEs associated with UAV-OBS, in general. Here, $r <$ h$_u$tan(ϕ).

IV. Simulation Results

The performance of different heterogeneous network configurations has been analyzed along with demonstrating the coverage region of each base station in the network. We compare the two network configurations for (i) one UBS and one MBS network, and (ii) two UBS and one MBS network. Specifically, two network configurations are investigated: (i) Heterogeneous network with MBS and UAV-CBS, and (ii) Heterogeneous network with MBS and UAV-OBS. Further, we also analyzed the performance of the heterogeneous network with MBS and opportunistic cellular/VLC at UBS. In this case, the UBS can serve as either CBS or OBS, depending on the UE's requirement and location.

We assume that the heterogeneous network covers an area of 2 km $\times$ 2 km. The region is discretized into 200 $\times$ 200 locations. Each location has the same size of 10 m $\times$ 10 m. The MBS is located at $\langle$ 0 m, 1 km $\rangle$ 2D coordinates, and the altitude of the MBS is 30 m. Further, the total transmit power (including MBS and UBSs) remains constant throughout the analysis for a fair comparison. Other simulation parameters are listed in Table I.

A. One UBS and One MBS

For the given parameters, we can find the optimal UBS location, for both cellular and VLC based transmission, using section-III. For effective comparison, we compare the most effective scenario of different configurations. Fig.2(a) shows the trace of the UAV-CBS's movement to find an optimal location as described in section-III(A). UAV-CBS shall be placed at $\langle$-0.6,-0.005$\rangle$ for maximum average received spectral efficiency. Fig. 2(b) shows the how average received spectral efficiency varies with the position of UAV-OBS to find the optimal location as described in subsection III.B. As we can see in Fig. 3, UAV-OBS performs equally well at coordinate(s) $\langle$-0.7, $\upsilon\rangle$ $\forall$ υ ϵ $\langle$-0.75, 0.75$\rangle$. For simplicity, keeping y-coordinate as 0, the UAV-OBS shall be placed at $\langle$-0.7, 0$\rangle$ and for the maximum average received spectral efficiency.

Fig.4 shows the locations associated with UBS and MBS in three different configurations. In Fig. 4(a), we can observe that UAV-CBS can cover around 40% of the region. We also have received the average spectral efficiency of 14.2 bps/Hz. Only about 10% of the region is under the UAV-OBS association, as per Fig.4(b). As per (2), the NLOS probability increases with the distance. NLOS significantly reduces the received SNR from UAV-OBS to UEs. Thus, UEs, in NLOS, associate with the MBS instead of UAV-OBS. An important

Table I
Simulation Parameters

Parameter	Symbol	Value
Carrier Frequency	f_c	2GHz
Environmental Parameter	α	11.9
Environmental Parameter	β	0.13
Excessive Pathloss LOS	ξ_{los}	6dB
Excessive Pathloss NLOS	ξ_{nlos}	26dB
MBS transmission power	p^m	46 dBm
UBS transmission power	p^u	30 dBm
Noise power	σ_1^2	-104 dBm
Altitude of UBS	h^u	200 m
Altitube of MBS	h^m	30 m
Free space ref. distance	d_o	100 m
LOS threshold	Γ	0.6
Refractive index n	μ	1.5
Optical filter gain	T_s	1
Wall reflection	ϱ	0.8
LED irradiance angle	ϕ	60°
FOV of receiver	$\psi_\rfloor$	60°.
Responsivity	$\mathcal{R}$	0.5 $\frac{\text{A}}{\text{W}}$

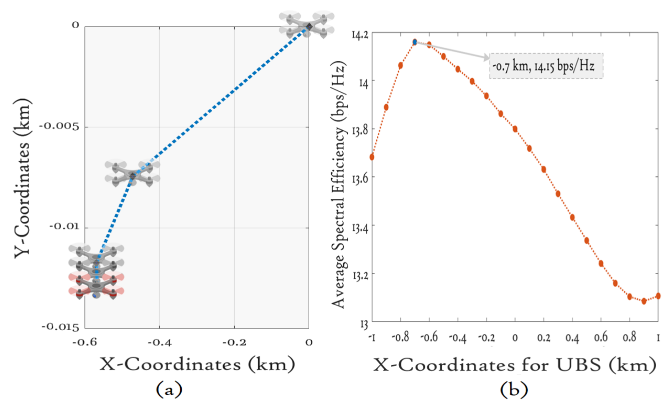

Figure 2. (a) Trace of the UAV-CBS's movement on each iterative step to find UBS location as described in section-III.A. (b) Average received spectral efficiency v/s position of the UAV-OBS to find UBS location as described in subsection III.B

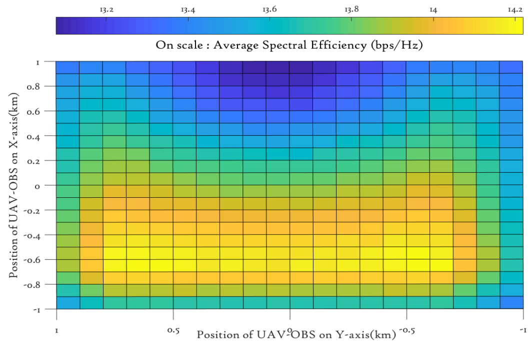

Figure 3. Average spectral efficiency received for various x-y position coordinates of UAV-OBS in Heterogeneous network with MBS

point to note is that these 10% UEs are now associated with the unlicensed visible light band. Thus, the limited licensed cellular band is now divided into the rest 90% users, improving the channel capacity per user by 1.1x. The received spectral efficiency of this network configuration is found out to be 14.15 bps/Hz. Though intuitively the UEs were expected to get better performance in the UAV-OBS case, it is not so. This is because the reachability of UAV-OBS is very limited. This causes many users, on the cell edge and region boundary, to receive poor SNR than the case with UAV-CBS. Thus, on average, the performance degrades a bit.

While analyzing the various network configuration as discussed above, we tend to notice that while UAV-OBS help in decreasing load on the licensed band, UAV-CBS has better reachability and coverage. To address both the concerns together, we can use the heterogeneous network with MBS and an opportunistic RF/VLC at UBS. Thus, UAVs should act as either UAV-CBS or UAV-OBS depending on the UEs position, LOS probability, and SNR-based association. We, thus, can achieve 10% better performance as compared to the previous two cases, with spectral efficiency around 15.56 bps/Hz.

B. Two UBS and One MBS

To get a holistic view of the performance metrics in the heterogeneous networks, we analyzed how one additional UBS will add to the efficiency of the network. Fig.5 shows the locations associated with two UBS and MBS in three different configurations. Note that, in the case of using multiple UAV-OBS, there might be interference from the neighboring UBS using VLC. The impact of such interference is minimized by optimally locating the UBS such as no user is in FOV of two UBS in an instance. Since the user is not in the FOV of the interferer, the interference power is very less and thus can be neglected. Thus, we chose the location of two UAV-OBS as two farthest points as shown in fig.3 for which the heterogeneous network performs best. That is, $\langle$ -0.7,-0.75 $\rangle$ for UAV-OBS1 and $\langle$ -0.7,0.75 $\rangle$ for UAV-OBS2. For, UAV-CBS, we opt to choose the position of UBS to maximize the percentage of the region associated with UAV-CBS and thus, improving the overall performance. Using simulations, chose

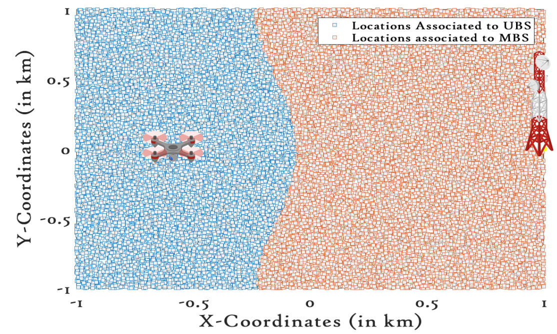

(a) Heterogeneous network with one MBS and one UAV-CBS

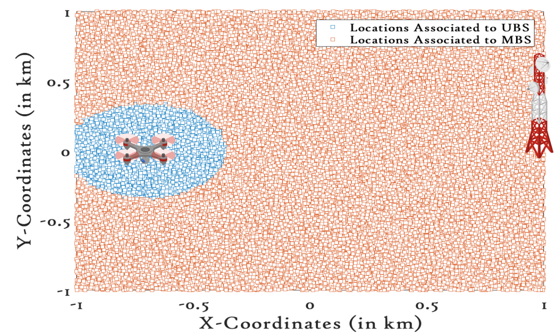

(b) Heterogeneous network with one MBS and one UAV-OBS

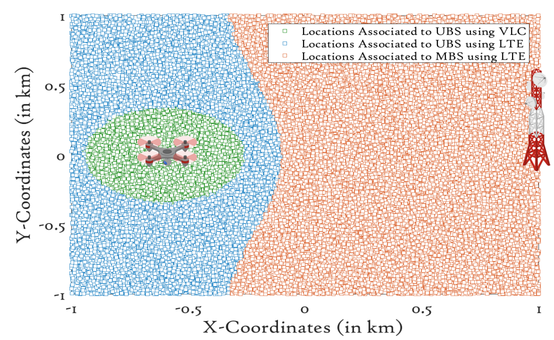

(c) Heterogeneous network with one MBS and opportunistic RF/VLC at a UBS location

Figure 4. Association map showing the locations under one UBS and one MBS association for different network configuration.

the location as $\langle$ 0.6,0.6 $\rangle$ for UAV-CBS1 and $\langle$ 0.6,-0.6 $\rangle$ for UAV-CBS2. At this location set, each UAV-CBS associates to 25% area and there is no location in the association region of more than one UAV-CBS.

In Fig.5(a), we observe that almost 50% of the location is associated with UAV-CBS. We received spectral efficiency of around 15 bps/Hz which is a slight improvement over the network with 1 UAV-CBS. Now, the performance of 2 UAV-OBS and 1 MBS is shown in Fig.5(b). A total of 20% users are now served using VLC access links via UAV-OBS. Thus, the limited licensed cellular band is now divided into the rest 80% users, improving the channel capacity per user by 1.25x. The average received spectral efficiency gets to around 16.5 bps/Hz. This is a significant increase w.r.t using two

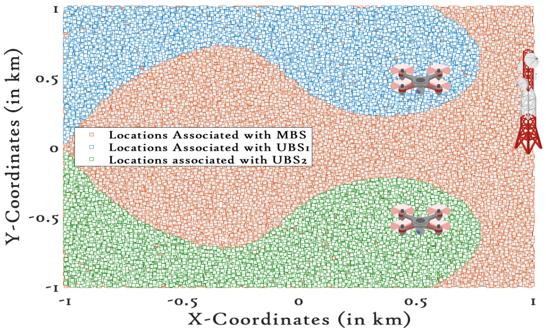

(a) Heterogeneous network with one MBS and two UAV-CBS

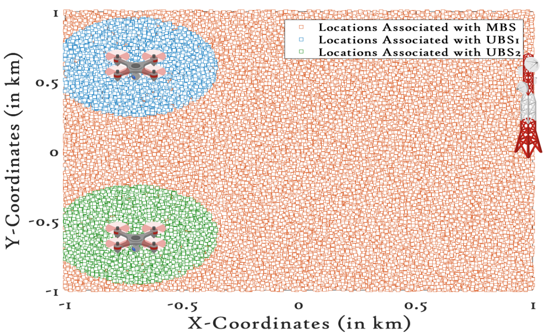

(b) Heterogeneous network with one MBS and two UAV-OBS

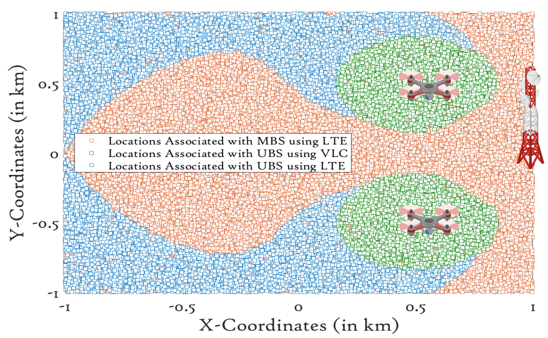

(c) Heterogeneous network with one MBS and opportunistic RF/VLC at a UBS location

Figure 5. Association map showing the locations under two UBS and one MBS association for different network configuration.

UAV-CBS. As discussed for one UBS and one MBS network, we now can look for improvement by using a heterogeneous system with an opportunistic cellular/VLC at UBS. As shown in fig.5(c), around 60% of locations can be served using UBS. Around one-third of these locations are catered using the VLC channel. We noticed a 7% performance improvement than the previous case, with spectral efficiency around 17.65 bps/Hz.

V. Conclusion

We can infer, from the simulation results, that as the number of UAVs in use increases, the network with VLC enabled UBS performs much better than cellular enabled UBS. This is because UAV-OBS helps us reduce the load over the licensed band. Moreover, using an opportunist cellular/VLC enables UBS to provide better efficiency and a user-centric approach to the problem. The framework and analysis can be used to help the network operator chose the suitable configuration to serve the users better. As an extension to this work, we plan to statistically characterize the ideal distance between two UBS, enabling coordinating multipoint (CoMP) transmission, in the heterogeneous environment to further improve the performance of the network.

Acknowledgement

Authors will like to thank the Visvesvaraya research fellowship, Department of Electronics and Information Technology, Ministry of Communication and IT, Government of India, for providing financial support for this work.

References

[1] Arvind Merwaday and Ismail Guvenc. Uav assisted heterogeneous networks for public safety communications. In *2015 IEEE wireless communications and networking conference workshops (WCNCW)*, pages 329–334. IEEE, 2015.

[2] Mohammad Mozaffari, Walid Saad, Mehdi Bennis, and Mérouane Debbah. Unmanned aerial vehicle with underlaid device-to-device communications: Performance and tradeoffs. *IEEE Transactions on Wireless Communications*, 15(6):3949–3963, 2016.

[3] Mohammad Mahdi Azari, Fernando Rosas, Kwang-Cheng Chen, and Sofie Pollin. Joint sum-rate and power gain analysis of an aerial base station. In *2016 IEEE Globecom Workshops (GC Wkshps)*, pages 1–6. IEEE, 2016.

[4] Akram Al-Hourani, Sithamparanathan Kandeepan, and Abbas Jamalipour. Modeling air-to-ground path loss for low altitude platforms in urban environments. In *2014 IEEE global communications conference*, pages 2898–2904. IEEE, 2014.

[5] Qingqing Wu, Yong Zeng, and Rui Zhang. Joint trajectory and communication design for uav-enabled multiple access. In *GLOBECOM 2017-2017 IEEE Global Communications Conference*, pages 1–6. IEEE, 2017.

[6] Vishal Sharma, Mehdi Bennis, and Rajesh Kumar. Uav-assisted heterogeneous networks for capacity enhancement. *IEEE Communications Letters*, 20(6):1207–1210, 2016.

[7] Harald Haas, Liang Yin, Yunlu Wang, and Cheng Chen. What is lifi? *Journal of lightwave technology*, 34(6):1533–1544, 2015.

[8] Lifang Feng, Rose Qingyang Hu, Jianping Wang, Peng Xu, and Yi Qian. Applying vlc in 5g networks: Architectures and key technologies. *IEEE Network*, 30(6):77–83, 2016.

[9] Ahmad Helmi Azhar, Tuan-Anh Tran, and Dominic O'Brien. A gigabit/s indoor wireless transmission using mimo-ofdm visible-light communications. *IEEE photonics technology letters*, 25(2):171–174, 2012.

[10] Michael B Rahaim, Anna Maria Vegni, and Thomas DC Little. A hybrid radio frequency and broadcast visible light communication system. In *2011 IEEE GLOBECOM Workshops (GC Wkshps)*, pages 792–796. IEEE, 2011.

[11] Xiang Sun, Nirwan Ansari, and Rafael Fierro. Jointly optimized 3d drone mounted base station deployment and user association in drone assisted mobile access networks. *IEEE Transactions on Vehicular Technology*, 69(2):2195–2203, 2019.

[12] Akram Al-Hourani, Sithamparanathan Kandeepan, and Simon Lardner. Optimal lap altitude for maximum coverage. *IEEE Wireless Communications Letters*, 3(6):569–572, 2014.

[13] Anand Singh, Gourab Ghatak, Anand Srivastava, Vivek Ashok Bohara, and Anand Kumar Jagadeesan. Performance analysis of indoor communication system using off-the-shelf leds with human blockages. *IEEE Open Journal of the Communications Society*, 2:187–198, 2021.

[14] Yash Gupta, Anand Singh, Ashutosh Bansal, Vivek Bohara, and Anand Srivastava. Deploying visible light communication for alleviating light pollution. In *2020 IEEE International Conference on Advanced Networks and Telecommunications Systems (ANTS)*, pages 1–4. IEEE, 2020.